ELSEVIER

Spectrochimica Acta Part A 51 (1995) 1517–1524

SPECTROCHIMICA
ACTA
PART A

Spectroscopic study of the isomerization of *Z*- to *E*-pyridine-2-formyl thiosemicarbazone

M.L.A. Temperini *, M.R. dos Santos, V.R. Paoli Monteiro

Instituto de Química da Universidade de São Paulo, C.P. 26.077, 05599-970 São Paulo, SP, Brazil

Received 27 October 1994; accepted 7 November 1994

Abstract

Pyridine-2-formyl thiosemicarbazone (PATS2) was synthesized in the *E* (anti) and *Z* (syn) configurations. Raman spectra were obtained in the solid state, and in DMSO and aqueous solutions. The SER spectra of PATS2 adsorbed on a silver electrode in DMSO and in aqueous solutions showing striking differences. The comparison of Raman data revealed that PATS2 is present on the silver electrode surface in the same configuration as the predominant isomer of the corresponding parent solutions. The prevalence of the *E* (anti) isomer in DMSO solutions was confirmed by Raman and ^{1}H NMR spectroscopies, and by means of the latter technique, the anti configuration is also proved to be predominant in aqueous solutions of different pHs, even starting with *Z*-PATS2 solutions. A strong interaction of *E*-PATS2 with water molecules by hydrogen bonding accounts for marked differences in Raman spectra of this isomer in DMSO and water solutions, and for the corresponding *E*-PATS2 species adsorbed on the silver electrode surface.

1. Introduction

One of the goals in current electrochemical research concerns the elucidation of adsorption reaction mechanisms at electrode surfaces. This can be achieved by coupling conventional electrochemical experiments to molecule-specific spectroscopic methods.

Pyridine-2-formyl thiosemicarbazone (PATS2) has been used to chemically modify the gold electrode surface [1]. This compound presents two geometrical isomers, *E*- and *Z*-PATS2 (Fig. 1). Hill and co-workers concluded from electrochemical data, that PATS2 is present in the *Z* (syn) configuration on a gold electrode in aqueous medium and that this configuration is changed by the nature of the electrolyte anion [2].

Previously, NMR results of PATS2 in DMSO-d_6 solutions have shown *E*-PATS2 as the predominant species in that solvent [3]. As Hill and co-workers concluded that PATS2 adsorbs on a gold electrode in the *Z* configuration they proposed two different adsorption mechanisms to explain the apparent discrepancy: (i) a selective adsorption of *Z*-PATS2 from PATS2 solution; (ii) adsorption of *E*-PATS2 with concomitant isomerization at the electrode surface.

---

* Corresponding author.

SSDI 0584-8539(94)01317-2

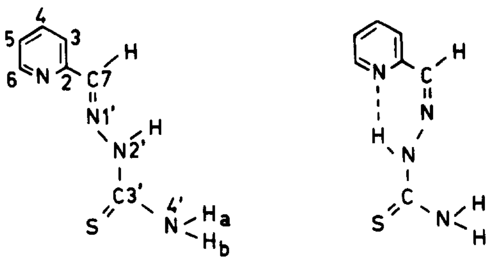

E - PATS 2 Z - PATS 2

Fig. 1. Chemical structure of *E*- and *Z*-PATS2.

Using SER spectroscopy, we characterized the adsorption of pyridine-4-formyl thiosemicarbazone (PATS4) and PATS2 on a silver electrode in aqueous medium and proposed that the hydrazone group and sulfur atom are the surface binding sites of the PATS*n* compounds [4]. The SER spectra of adsorbed PATS2 were very sensitive to the electrolyte anion, pH of the solution and applied potential. The interpretation of these spectra was done based on the existence of *E* and *Z* geometric isomers on the surface [4,5].

The goal of the present work is to give some additional insight into the adsorption mechanism of *E*-PATS2 on silver electrodes in aqueous solution. Raman and NMR techniques were used for establishing the preferential PATS2 configuration both in solution and in the solid state. These data are compared to those obtained for a PATS2-modified silver electrode in aqueous and DMSO solutions. The results lead to a new interpretation of the configuration of adsorbed PATS2.

2. Experimental

PATS2 was synthesized as described in Ref. [3]. The purity of the compound was checked by elemental analysis and the predominance of the *E*-PATS2 isomer was confirmed by TLC and NMR.

Z-PATS2 isomer was prepared by heating a dried methanol solution of *E*-PATS2 with SiO_2 in a rotoevaporator at 50 °C for 4 h. Thereafter, the solvent was evaporated and the residue was extracted with freshly distilled ethyl acetate. The compound was purified by chromatography using a silica gel column and ethyl acetate as eluant. The purity of *Z*-PATS2 was confirmed by TLC and NMR.

Raman and SER spectra were done on a Spex Triplemate-1877 fitted with an intensified diode array (an OMA-III-EGG-PAR detection system), using the 514.5 nm line from a 2020 Spectra Physics Ar^+ laser. Owing to some fluorescence, the FT-Raman spectra of *Z*-PATS2 were recorded on a Bomem DA3 spectrometer equipped with an FT-Raman accessory, an InGaAs detector and a quartz beamsplitter. The FT-Raman spectra were excited with the 1064 nm line from an Nd–YAG laser operated at 200 mW. All samples were placed in glass capillary tubes.

The details of the SERS cell and the experimental conditions used in the measurements have been published elsewhere [4]. The working electrode was a 0.13 cm^2 polycrystalline silver (99.99%) plate supported by a shrinkable tubing from Alpha Wire Corporation. Prior to each experiment, the working electrode was polished mechanically with 600-mesh sandpaper and rinsed with distilled water and then with DMSO when necessary. The auxiliary and reference electrodes were a large area platinum sheet and saturated calomel electrode (SCE), respectively.

Reagent grade KCl and tetramethylammonium chloride $[(CH_3)_4NCl]$ were used as supporting electrolytes. The solutions were prepared with double distilled water or DMSO dried over molecular sieves. Oxidation–reduction cycles were applied to the silver electrode in 0.1 M KCl/H_2O or 0.1 M $(CH_3)_4NCl/DMSO$ solutions containing

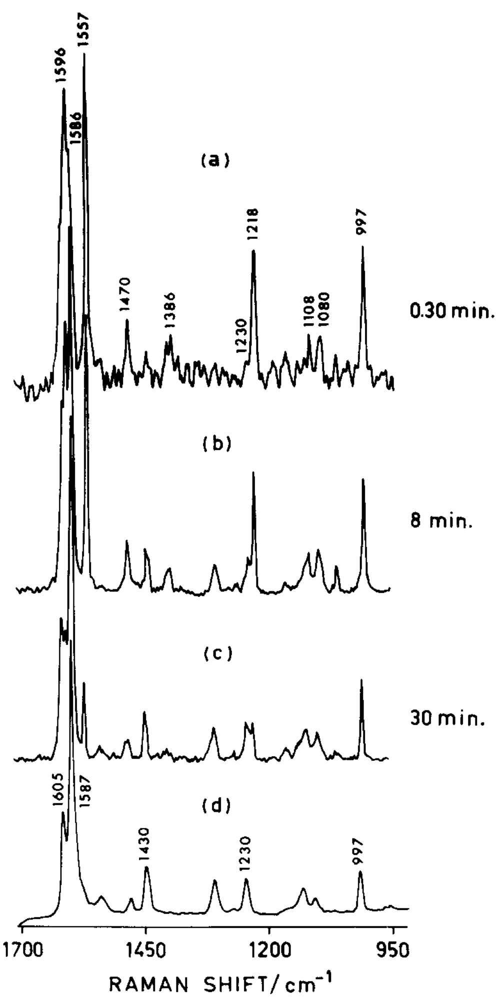

Fig. 2. (a–c) Dependence of the FT-Raman spectra of Z-PATS2 in the solid state on the exposure time to laser radiation ($\lambda = 1064$ nm). (d) Raman spectrum of E-PATS2 in the solid state ($\lambda = 514.5$ nm).

E-PATS2, with concentrations of 10^{-5} M in aqueous solutions and 2.0×10^{-3} M in DMSO. Cyclic voltammograms were obtained using a PAR 273 potentiostat/galvanostat.

^{1}H NMR spectra were taken on a Brüker AC-200 spectrometer in FT-mode (pulse width = 8 μs, acquisition time = 2.56 s, relaxation delay = 0, number of scans = 128). Frequencies were measured either with respect to internal TMS (DMSO-d_6 solutions) or internal 3-(trimethylsilyl)1-propanesulfonate (D_2O solutions) at room temperature, and chemical shifts were calculated using the iterative program UEAITR [6] adapted for personal computer (IBM compatible) [7].

3. Results and discussion

Fig. 2a–c shows the FT-Raman spectra of PATS2 synthesized in the Z configuration in the solid state. The sequence of the presented Raman spectra shows the spectral changes with the exposure time (indicated in each spectrum) of the sample to the exciting radiation. In order to follow the temporal evolution of the Raman intensities, data acquisition was restricted to a few scans. One can see that the most prominent bands, at 1596, 1557, 1470, 1386 and 1218 cm^{-1}, decrease in intensity as the excitation time increases. The opposite is observed for the bands at 1605, 1586, 1430 and 1230 cm^{-1}. These latter bands can be seen in the spectrum of E-PATS2 (Fig. 2d), suggesting that there is a Z to E isomerization during the FT-Raman measurements.

Fig. 3 shows the dependence of the FT-Raman spectra of *Z*-PATS2 in DMSO solution on the exposure time (indicated in each spectrum) to laser radiation. Again, the Raman bands characteristic of *E*-PATS2 increase in intensity as the exposure time increases, suggesting that the isomerization of *Z*- to *E*-PATS2 also occurs in DMSO solution.

Fig. 4 shows the Raman spectra of PATS2 synthesized in the *E* configuration in solutions of different DMSO–water ratios. The Raman spectrum of the solvent (DMSO or DMSO–water) was subtracted from each spectrum, sometimes resulting in negative-going bands. A large change in the relative intensity of the bands is observed and almost all bands present a shift to higher frequencies when water is added to the *E*-PATS2/DMSO solution. Besides the relative intensity changes and frequency shifts, a new feature emerges at 1565–1569 cm^{-1}. The origin of this feature will be addressed later. These results suggest either a strong interaction between *E*-PATS2 and water, or an isomerization of *E*-PATS2 to *Z*-PATS2 in this solvent, in agreement with the assumption of Beraldo and Tosi [8]. From the UV–vis and pre-resonance Raman behavior of *E*-PATS2 in aqueous solutions at different pHs, these authors proposed the isomerization of *E*- to *Z*-PATS2 in solutions of $6.5 < \mathrm{pH} \leqslant 10$. Below or above these limits they assumed that PATS2 is in the *E* configuration.

Since the Raman technique showed a high sensitivity for detecting changes in the nature of the species, we decided to obtain the SER spectra of PATS2 adsorbed on a silver electrode in DMSO and water solutions.

The SER spectrum of a silver electrode in 0.1 M $(CH_3)_4NCl$ + DMSO solution containing PATS2 synthesized in the *E* configuration (Fig. 5a) shows significant differences in relation to the SER spectrum of a silver electrode in 0.1 M KCl aqueous solution containing *E*-PATS2 (Fig. 5b). The SER spectrum of a silver electrode in DMSO containing *E*-PATS2 (Fig. 5a) shows a strong resemblance to that obtained in DMSO solution (Fig. 4a). The main differences are changes in relative intensities and a new Raman feature appearing at 1500 cm^{-1}. The same similarity is seen between the SER spectrum of a silver electrode in aqueous solution containing *E*-PATS2 (Fig. 5b) and the Raman spectrum of *E*-PATS2 in water (Fig. 4c).

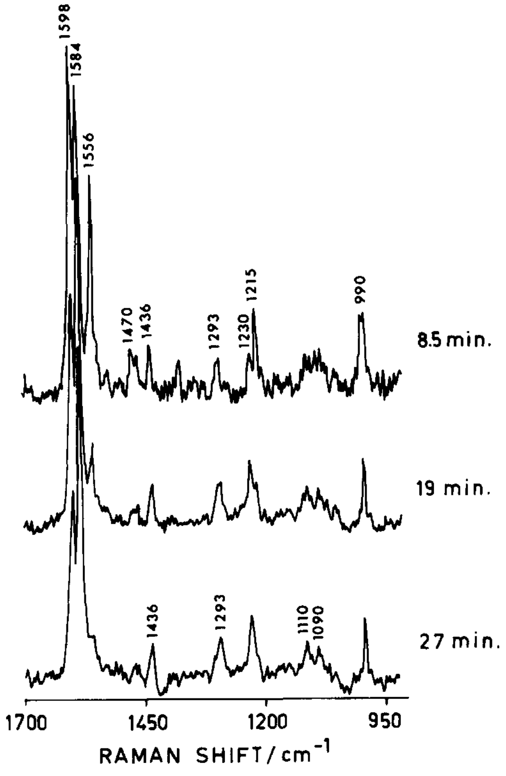

Fig. 3. Same as Fig. 2, but for *Z*-PATS2 in DMSO solution.

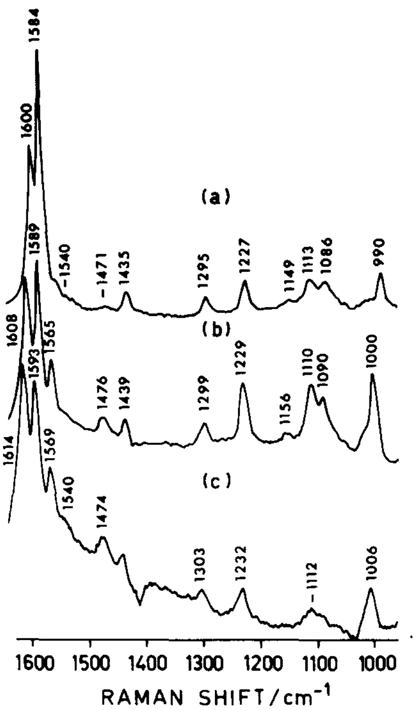

Fig. 4. Raman spectra of *E*-PATS2 in: (a) DMSO; (b) 75% DMSO + 25% water; (c) water + 5% DMSO ($\lambda = 514.5$ nm).

These results strongly suggest that PATS2 adsorbs on a silver electrode with the same configuration it has in the solvent being used, thus excluding the initial hypothesis of selective adsorption of the minor isomer in solution, as well as adsorption with concomitant surface isomerization proposed earlier [2].

The question concerning the configuration of the major component of PATS2 in water will be studied using NMR spectroscopy.

^{1}H NMR studies performed by Karabatsos and co-workers have shown that formyl protons of thiosemicarbazones in the *E* (anti) configuration resonate at lower magnetic fields than in the *Z* (syn) configuration, regardless of the solvent [9]. On the basis of these results, Antonini and co-workers synthesized PATS2 isomers and concluded that the *E* (anti) configuration is the predominant one in DMSO solutions of PATS2 [3], which is

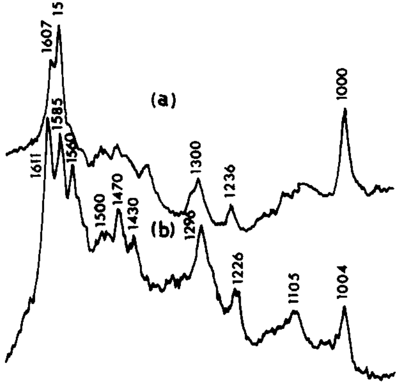

Fig. 5. SER spectra of a silver electrode at −0.2 V in: (a) DMSO/0.1 M $(CH_3)_4NCl/5 \times 10^{-2}$ M *E*-PATS2; (b) water/0.1 M KCl/5×10^{-3} M *E*-PATS2 ($\lambda = 514.5$ nm).

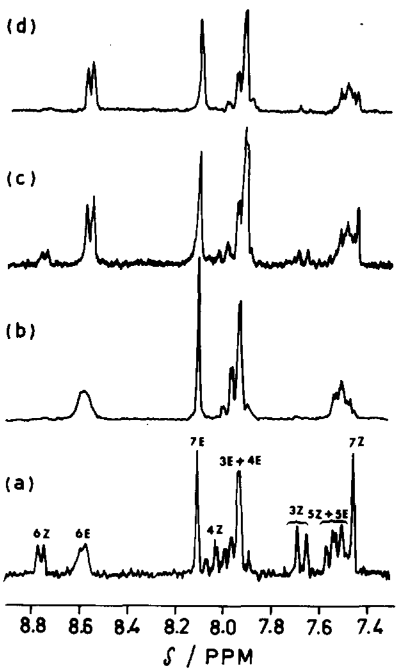

Fig. 6. ^1H NMR spectra of Z-PATS2 in D_2O solutions: (a) after 20 min of preparation of solution, showing Z to E isomerization; (b) after 2 h in solution; (c) after 20 min in solution at pH 8.0; (d) after 1 h and 30 min in solution at pH 8.0.

also corroborated by the Raman data presented in this work. Unfortunately, no reference to a ^1H NMR study of PATS2 in water was found.

In order to verify the configuration PATS2 will preferentially assume in water, the ^1H NMR spectra of E- and Z-synthesized PATS2 in D_2O solution were obtained.

Fig. 6 shows the ^1H NMR spectra of Z-PATS2 after about 20 min (a) and 2 h (b) of preparation of solution. Note that the signal-to-noise ratio in the spectrum of Fig. 6a is poor owing to the small number of scans used to obtain it. However, these conditions allowed us to follow the isomerization process. The main features in the spectrum of Fig. 6a are the two singlets at 8.10 and 7.46 ppm due to formyl protons of the E (anti) and Z (syn) configurations, respectively. Note that after 2 h (Fig. 6b), the 7.46 ppm peak and others related to Z-PATS2 disappeared, i.e. only one isomer is present in the solution, E-PATS2. It is worth mentioning that the initial purity of Z isomer was checked in DMSO-d_6 solution, showing the presence of no more than 15% of E isomer.

The experiment was repeated at various pH values (from 1 to 13) and the spectrum of the E isomer always developed from the initial ones. Fig. 6c and d illustrates this behavior at pH 8.0.

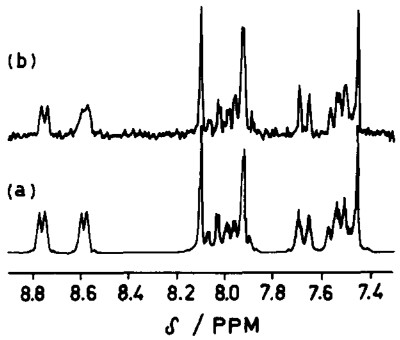

Fig. 7. (a) ^1H NMR spectrum calculated by iterative curve for a 50%/50% mixture of Z- and E-PATS2 in D_2O. (b) The same spectrum as Fig. 6a, to which the calculated spectrum was fitted.

Table 1
PATS2 proton chemical shifts (δ/ppm)

Config.	Solvent	3	4	5	6	7	2′	4′
E	DMSO-d_6	8.27	7.82	7.37	8.56	8.08	11.63	8.34/8.17
Z	DMSO-d_6	7.79	8.09	7.57	8.79	7.43	14.04	8.58/8.24
E	D_2O/pH 6.0	7.92	7.95	7.50	8.58	8.10	–	–
Z	D_2O/pH 6.0	7.67	8.02	7.54	8.76	7.46	–	–
E	D_2O/pH 8.0	7.91	7.94	7.49	8.57	8.10	–	–
Z	D_2O/pH 8.0	7.67	8.02	7.53	8.75	7.45	–	–

In Fig. 7a, the ^1H NMR spectrum calculated for a mixture of 50% *Z*- and 50% *E*-PATS2 is presented. Calculated spectra of *Z* and *E* isomers were iterated separately (by curve fitting) and summed using a line broadening of 1.7 Hz and 1:1 intensity ratios. For comparison, Fig. 7b shows the same spectrum of Fig. 6a that was used in the fitting procedure.

Table 1 presents the chemical shifts of protons of *E*- and *Z*-PATS2 at pH 6.0 and 8.0, and the chemical shifts of both species in DMSO-d_6. Table 2 presents the chemical shifts of aromatic protons 4 and 5 in various solutions. We observe that as the pyridine nitrogen becomes more involved in stronger hydrogen bonding, these protons are shifted to lower field until the $N-H^+$ bond is formed at low pH [10].

In D_2O solution, the replacement of the deuterium atoms for N(2′)H and N(4′)H_2 occurs for both *E*- and *Z*-PATS2 isomers, showing the lability of the N(2′)H–N intramolecular hydrogen bonding of *Z*-PATS2 in water. During these chemical exchange processes, the intermediate formed should have less restricted C=N bond rotation in order to allow the *Z* to *E* conversion, and once the anti isomer is formed, it is stabilized by intermolecular hydrogen bonding with water molecules. It is worth mentioning that an X-ray crystallographic investigation of *E*-PATS2 [11] showed that two molecules are linked into a dimer by hydrogen bonding through the thioamide groups. This dimer is further reinforced by hydrogen bonding involving two water molecules, thus showing that intermolecular hydrogen bonding interactions may be more advantageous over intramolecular hydrogen bonding concerning the stabilization of PATS2 molecules.

Therefore, the *E* (anti) configuration of PATS2 is predominant in aqueous solutions at any pH. As *E*-PATS2 is also the predominant isomer in DMSO, the dramatic Raman spectral changes of *E*-PATS2 with addition of water to DMSO solutions are confirmed to be due to hydrogen bonding between *E*-PATS2 and water. It has to be stressed that although the band at 1569 cm^{-1} (Fig. 4c) lies in the region of amide II vibration, by using D_2O as solvent there is no decrease in its relative intensity. Therefore, a possible explanation for the origin of this feature is a breakdown of the coupling between the pyridine ring stretching vibrations and the CN(1′) stretching mode due to the interaction of the molecule with water.

Table 2
Chemical shifts of protons 4 and 5 of *E*- and *Z*-PATS2 in different media (δ/ppm)

Config. Medium	*E* DMSO-d_6	*E* D_2O	*E* D_2O	*E* D_2O	*E* D_2O	*Z* D_2O	*Z* DMSO-d_6	*E* D_2O
pH	–	13.0	11.0	8.0	6.0	6.0	–	1.0
H(4)	7.82	7.91	7.91	7.94	7.95	8.02	8.09	8.64
H(5)	7.37	7.43	7.44	7.49	7.50	7.54	7.57	8.05

4. Conclusions

The present results show that *Z*-PATS2, in the solid state or in solution, is converted to *E*-PATS2. The predominant PATS2 species in DMSO and aqueous solutions is always the *E*-configuration, whatever the pH of the aqueous solution, and this is also the isomer adsorbed on the silver electrode surface, contradicting earlier interpretations [4,5,8], as well as the proposed adsorption mechanism [1,2]. The spectral differences between *E*-PATS2 adsorbed on silver electrodes in DMSO and in aqueous solutions can be explained by intermolecular hydrogen bonding of the *E* isomer to water molecules.

Acknowledgments

This work was supported by PADCT and BID/USP. M.L.A.T. and V.R.P.M. are indebted to CNPq for the grant of a fellowship, and M.R.S. to FAPESP. The authors thank Luiz Carlos Roque from Central Analítica (IQUSP) for NMR spectra.

References

[1] H.A.O. Hill, D.J. Page and N.J. Walton, J. Electroanal. Chem., 217 (1987) 129.

[2] H.A.O. Hill, D.J. Page and N.J. Walton, J. Electroanal. Chem., 208 (1986) 395.

[3] I. Antonini, F. Claudi, P. Franchetti, M. Grifantini and S. Martelli, J. Med. Chem., 20 (1977) 447.

[4] L.S. Pinheiro and M.L.A. Temperini, J. Electroanal. Chem., 295 (1990) 169.

[5] L.S. Pinheiro and M.L.A. Temperini, Proceedings of the XXII International Conference on Raman Spectroscopy, Columbia, SC, (edited by J.R. Durig and J.F. Sullivan), p. 232 (1990).

[6] R.B. Johannesen, J.A. Ferretti and R.K. Harris, J. Magn. Reson., 3 (1970) 384.

[7] F.Y. Fujiwara, personal communication.

[8] H. Beraldo and L. Tosi, Inorg. Chem. Acta, 125 (1970) 1397.

[9] G.J. Karabatsos, F.M. Vane, R.A. Taller, N. Hsi, J. Am. Chem. Soc., 86 (1964) 3351.

[10] V.M.S. Gil and J.N. Murrell, Trans. Faraday Soc. 60 (1964) 248.

[11] V.N. Biyushkin, Y.M. Chumakov, N.M. Samus and I.D. Baka, J. Struct. Chem., 28 (1987) 119.